Electron - pion separation in the ATLAS Tile hadron calorimeter

M. Simonyan

Yerevan Physics Institute, Yerevan, Armenia

Abstract

The ATLAS hadron Tile Calorimeter performance has been extensively studied during the test beam periods at the CERN SPS accelerator. The SPS beams contain the mixtures of the electrons, muons and pions, but for the physics studies it is important to deal with the pure beam species. Several methods of electron - pion separation were comparatively studied in this note, using available test beam data and detailed Monte Carlo simulation.

Introduction

An excellent particle identification capability is required at LHC for the most physics studies. Calorimeters, in conjunction with the other ATLAS sub-detectors can provide useful information for particle identification.

The methods of electron - hadron separation are generally based on the scale difference of electromagnetic and hadronic showers. The electromagnetic shower is relatively more compact and few cells of the calorimeter usually have a noticeable response. This fact is usually used as a separation criteria, but with different success, depending on the choice of the appropriate observable, relevant for the selected calorimeter structure. The methods of electron - pion separation, developed mostly for calorimeters with fine segmentation, as compared to the scale of electromagnetic showers are less efficient for the coarse granulation case like Tile Calorimeter(Tilecal). Since 1994 Tilecal community has used a few observables for electron - hadron separation, namely: difference in energy response of Tilecal to electrons and hadrons, due to its non-compensation, RMS of the energy response[1,3], the number of the hot cells [2], Ci-variable[4] as well as their combinations. In this note the capability of different methods, giving the most efficient electron - pion separation efficiency for Tilecal alone, is analyzed and compared.

The physics processes of prime interest of ATLAS require good energy response linearity and resolution to hadrons of the calorimeters over an unprecedented energy range. For non-compensating calorimeters like the ones of ATLAS this can be achieved

by an appropriate weighting technique. Some of the developed methods of electron – hadron separation are useful to tag the electromagnetic component of hadronic showers, which is crucial for the successful application of a weighting technique.

The electron - pion separation that one can achieve using calorimeter is limited by the underlying physical processes involved. If the charge-exchange reaction occurs in the first few radiation lengths of the calorimeter and almost all energy of the charged pion is transferred to the neutral one, then a purely electromagnetic shower will be generated. This shower is practically indistinguishable from those generated by the electrons, therefore such events could not be separated by any calorimeter information.

The structure of the note is the following.

In section 1 the event selection is described. The simulation tools are briefly presented in section 2. Electron/pion separation methods are described and analyzed in section 3. Their comparison is done in section 4.

1 Events selection

The electron runs for 50, 100, 180 GeV of the 2002 test beam period at pseudo-rapidity η = -0.35 have been selected for the analysis. A set of cuts was applied for the event selection. In order to eliminate the events with high angular spread in the beam, the wire beam chambers were used. The response of chambers was fitted with a Gaussian and 3 sigma cut applied on the beam profile. The MIP response is requested in the scintillator counters in order to select the single particle event. The random trigger events are used to define the noise threshold for each PMT. The noise is fitted with Gaussian and 3 sigma cut is applied. The calibration constants have not been used and energy is expressed in the units of pC. To avoid the muon events as well as the events with large leakage, 15, 30, 60 pC cuts on the total energy were used for 50, 100, 180 GeV runs respectively.

In order to compare the performance of different methods, the results of simulation, when reliable, are used to calculate electron - pion discrimination efficiency and misclassification.

2. Monte Carlo simulation tools

The simulation of the beam line and calorimeter modules was performed within ATHENA 11.0.1 framework with GEANT4 (geant4-07-01-patch-01) [5] using QGSP_GN 2.6 physics list. The default 1mm range cut has been used. Digitization was also done within the same ATHENA version. The noise was added at this stage to be equivalent to the test beam conditions. A simulation run with an artificial particle that do not leave energy in the calorimeter are used to define the noise cut for each PMT as it was done in case of the data using randomly triggered events.

The results obtained may also serve as a source of the GEANT4 validation, although that is not the prime goal of this note.

3 Data analysis and comparison with simulation

In the following, various observables are defined that can discriminate electrons from pions. Their performance will be assessed using the results of MC simulation of electrons

and pions, when reliable, or using a Gaussian distribution.

3.1 Total energy distribution

Since the Tilecal is a non-compensating calorimeter (e/h=1.36), electrons and pions can be separated using the calorimeter response itself. As the resolution of calorimeter is improved with energy as a $E^{-1/2}$, and the electromagnetic fraction of the hadron shower is scaled according to ln(E), the separation quality is improved with energy increase. The normalized energy distributions are shown in figure 1 for different beam energies together with MC simulation results. Since neither in the data nor in the MC the absolute scale is well determined, to compare simulations and data, a scale factor between data and MC has to be defined. The best agreement was found for the factor equal to 0.97 for all energies that was used afterwards. Since the true amount of electrons and pions in the beam is unknown, we tried to fit the relative amount of electrons and pions by adjusting the simulated distributions to the data such that hdata = w×helectron + (1-w)×hpions. However, no satisfactory description was obtained. The simulated distributions are broader than the one in the data both for electrons and pions. Moreover, for the pions, the more pronounced shift of the distribution leads to the failure of the fit.

Thus the data were fitted with the sum of simulated distribution for electrons and Gaussian function for pions. The results are shown in figure 1. The vertical lines show the fit region. It would be of course reasonable to make a fit in the energy range as wide as possible but due to larger widths of the simulated distributions the fit was restricted to the region between two peaks.

3.2 Number of the hot cells (Ncell)

A cell is taken into account if at least one of two PMTs has a signal higher than its noise cut, and the total cell signal is higher than 0.05 pC. The threshold was optimized to obtain a good separation for all energies. The experimental distributions are shown in fig 2 together with MC simulations. The left peak in the figures corresponds to electron events and the right one to pions. The result of the simulation of pions is also presented. As compared to the data, a shift is observed towards the low number of cells, that seems to be an indication that the simulated showers are compacter as compared to the experimental one. The same approach, as described above, is applied to fit the data. The similar observable was used for the analysis of the SPACAL calorimeter data [6].

3.3 Maximal density (MD)

The energy density in a cell is defined as the ratio of the energy deposit to the volume of the cells. All cells are scanned and a cell with maximum energy density is selected. The distributions of MD are presented in fig 3 together with the MC simulation results. As is seen from the figure, the simulation satisfactorily describes the maximum density data both for electrons and pions.

The first sampling of TileCal is appr. 14 X_o thick and electrons deposit most of their energy in one cell of the first sampling (A). A large fraction of the pions leaves most of its energy in one or two cells of the second sampling (BC) with the volume ratio appr. 4.5 times higher than in A one. The other part of the pions starts the shower earlier, with a

significant electromagnetic contamination in the first sampling. These two effects are clearly visible in the distribution of pions where the peak in the low density region corresponds to the second sampling while the tail in the high density region, to the one of the first sampling. The simulated results of MD for pions and electrons were used to fit the data. As before, the vertical lines in the figures show the fit region.

A similar observable, defined as a fraction of energy contained in the hot core of N contiguous cells, was used, for example, by H1 LAr calorimeter group[7].

3.4 Average density (AvD)

The average density is calculation as follows: a threshold for all cells was set proportionally to the total energy, event by event. All cells, with a signal above the threshold are used in the calculation of AvD:

$$AvD = \left(\sum_{i}^{Ncell} E_i / V_i \right) / Ncell$$

The distributions of AvD are presented in fig 4 together with the MC simulation results. The best quality of electron - pion separation was found for the threshold setting equal to 1% of the total energy in calorimeter, but not less than 0.05 pC. As one can see from the figure, the simulation of pions is not able to reproduce the experimental data satisfactorily. The simulation of electrons is more reliable and is used in conjunction with the Gaussian for the data fit.

An attempt to improve this method was made. The cells were given a weight equal to $1/r^2$ where r is the distance of the center of cells from the face of the calorimeter where beam hits. No noticeable improvement was observed that might be explained as follows. The late showering pion events (low density and low value of $1/r^2$) are already well separated from electrons and the factor $1/r^2$ shifts only those events to the left of the distribution of pions, while the early showering pions, which dominate in the right part (high density, high value of $1/r^2$), remain mixed with electrons.

3.5 C_i variable

This observable is usually defined as a fractional energy deposit in the first layer(s) of the calorimeter and was used, for instance, by H1 LAr calorimeter group[7]. In the Tile calorimeter [4] C_i variable is defined as

$$C_i = \sum_{j}^{Samplings 1,2} E_j / E_{beam}$$

a ratio of energy deposit in the first two samplings of Tilecal to the beam energy for the selected tower i. The distributions of C_i variable are shown in figure 5 with the results of MC simulation. In contrast to other methods described above, this observable uses the beam energy as an additional information, when the total energy is used, the separation efficiency decreases. The MC simulation of electrons and Gaussian function for the distribution of pions are used to fit the data.

4 Separation efficiency and misclassification

The determination of separation efficiency and misclassification was done by

extrapolating fit results into the region where the distributions of pions and electrons are mixed. For electrons this is a reliable procedure, due to the satisfactory quality of the MC simulation. The small difference between the widths of the simulation and the data will not noticeably affect the extrapolation to the range of the distribution of pions. In case of the pions, the extrapolation using a Gaussian, except for the MD observable, is used to evaluate the pion contamination in the distributions of the electrons. Figure 6 shows the electron separation efficiency versus contamination of pions at 180, 100, and 50 GeV runs for different methods. It is clearly seen that the AvD observable gives the best separation efficiency. In figure 7 the separation efficiency of pions versus contamination of electrons is plotted. The AvD observable again gives the best separation performance. Figure 8 shows the electron separation versus contamination of pions for all observables for different energies. In general the separation is improved towards growing energy as was mentioned above. The same result for pions is plotted in figure 9.

As it was mentioned above, the electron - pion separation methods exploit a different scale of electromagnetic and hadron showers. The ratio of corresponding nuclear interaction and radiation lengths is scaling proportionally to Z [8]. Therefore, a better separation efficiency can be achieved in calorimeters with higher Z absorber materials. Taking into account a higher Z value of absorber and a finer granularity of the ATLAS Electromagnetic Barrel Liquid Argon Calorimeter, one may expect a better performance for electron - pion discrimination as compared to Tilecal alone.

Conclusion

Various methods to separate electron from pions for the Tile calorimeter are analyzed in detail using Tilecal response only, without relying on the knowledge of beam energy. The experimental data are compared with the results of Monte Carlo simulations. The description of the data by the simulation is good for electrons, but not satisfactory for pions. The best separation efficiency has been achieved using the AvD observable, allowing to obtain 0.1% electron contamination for the 99% pion efficiency and 0.15% pion contamination for the 99% electron efficiency at 50 GeV. These results are obtained for particles impinging at a pseudo-rapidity of -0.35 that is close to the finest projective segmentation of Tilecal.

Acknowledgment

The author is thankful to his supervisors H. Hakobyan and A. Henriques for their help and support, as well as to T. Carli, I. Vichou and F. Spano for useful discussions and important comments. For the financial support the author greatly acknowledges the INTAS fellowship Ref. Nr. 04-83-2605 which gave him a chance of long term involvement in the Tilecal activity at CERN. Special acknowledgment to ATLAS spokesperson Peter Jenni for his personal support among other students from FSU countries.

References

[1] M. Bosman and A.Juste, The pion resolution and linearity, TILE-TR-41, Analysis meeting on the test beam data, 27 June 1995

[2] H. Hakopian and V.Grabsky. The pion uniformity in the z direction, TILE-TR-41, Analysis meeting on the test beam data, 27 June 1995

[3] R. Leitner Precise measurement of the energy loss spectrum of 180GeV muons in the iron absorber of the Tilecal Module 0, ATL-TILECAL-99-009

[4] Y. A. Kulchitsky, M. V. Kuzmin and V. B. Vinogradov Electron calibration of the TILECAL Module Cells, ATL-TILECAL-2001-002

[5] J. Agostinelli et al. GEANT4: A simulation toolkit, Nucl. Instrum. Meth. A 506 (2003) 250.

[6] D. Acosta et al., Electron-pion separation with a scintillating fiber calorimeter, Nucl.Instr.Meth. A302(1991)36-46

[7] B. Andrew et al., Electron - pions separation with the H1 Lar calorimeters, Nucl.Instr.Meth. A344(1994)492-506

[8] R. Wigmans, Calorimetry - Energy Measurement in Particle Physics, International Series of Monographs on Physics, vol. 107, Oxford University Press, Oxford, 2000

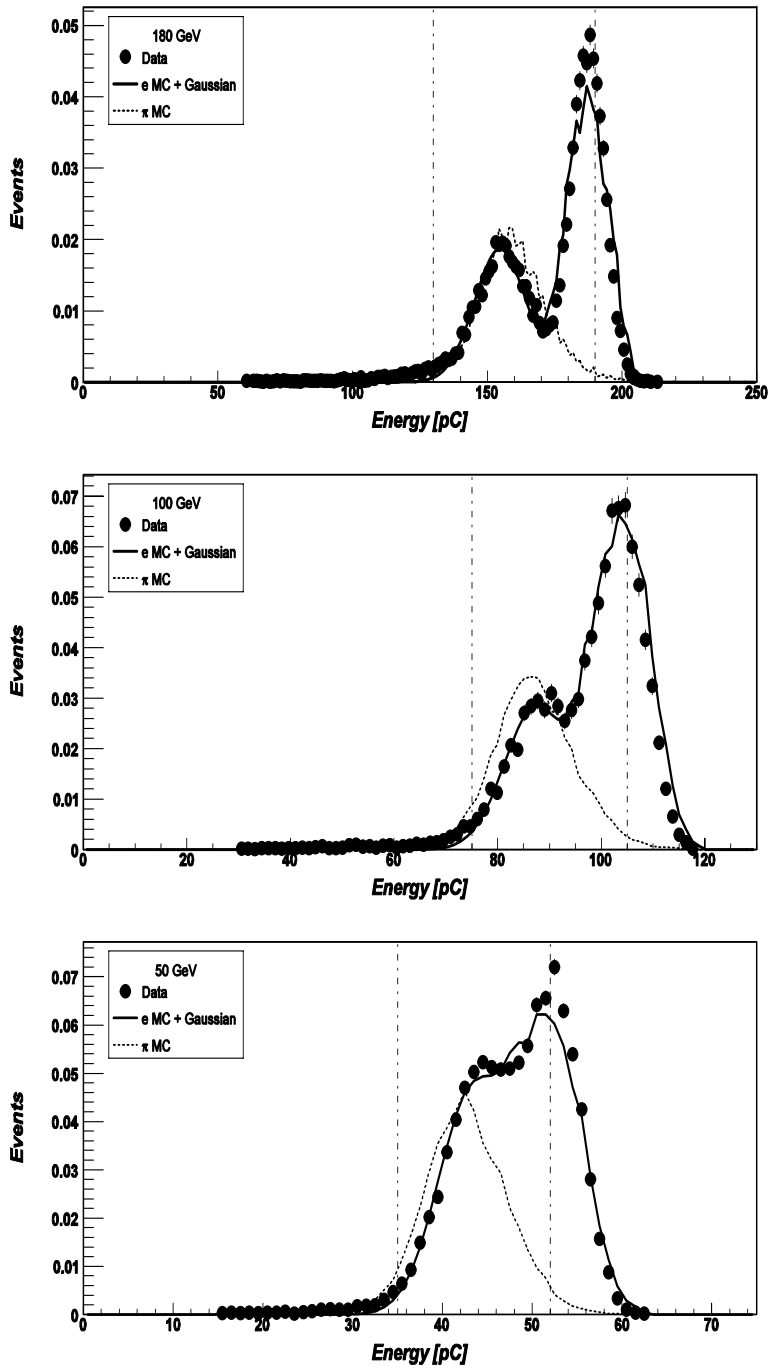

Fig.1 Normalized energy distribution for 180 (a), 100 (b) and 50 (c) GeV runs.

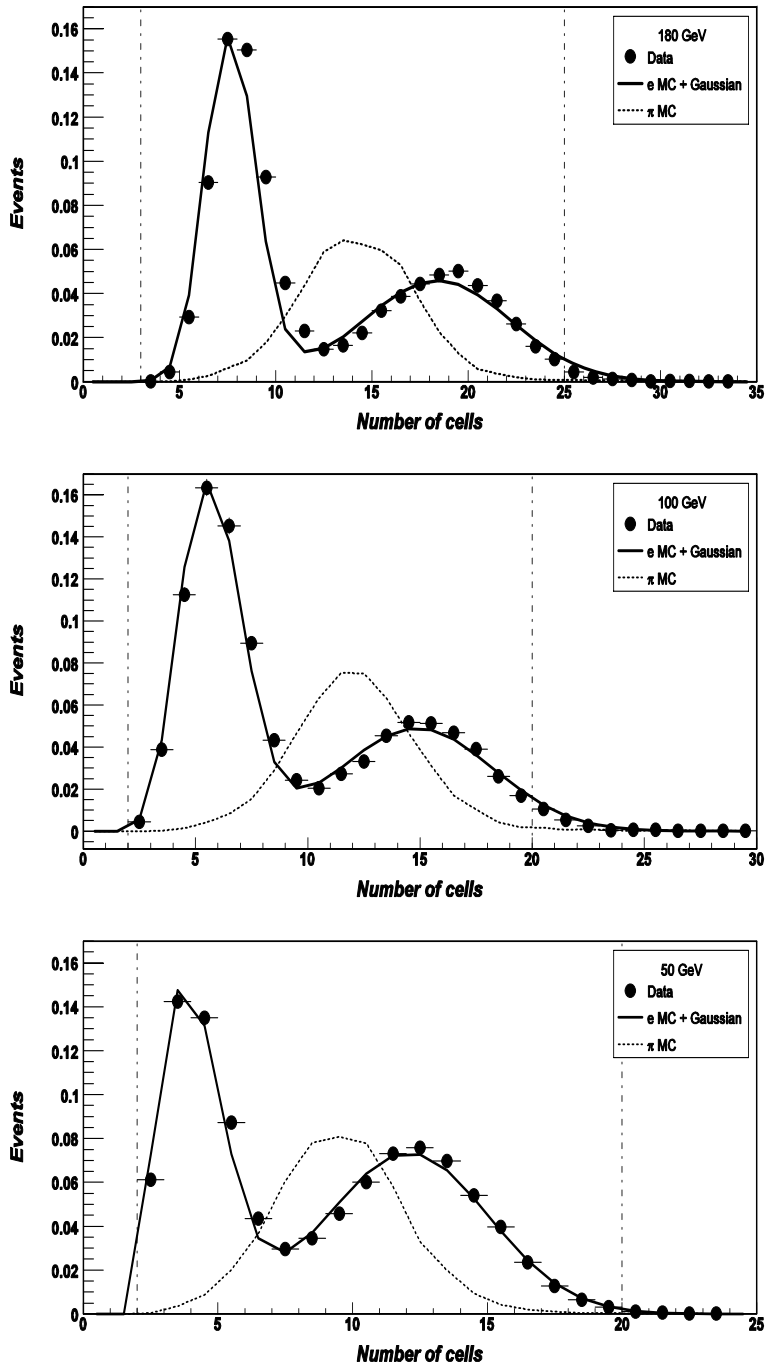

Fig.2 Normalized distribution of number of cells for 180 (a), 100 (b) and 50 (c) GeV runs.

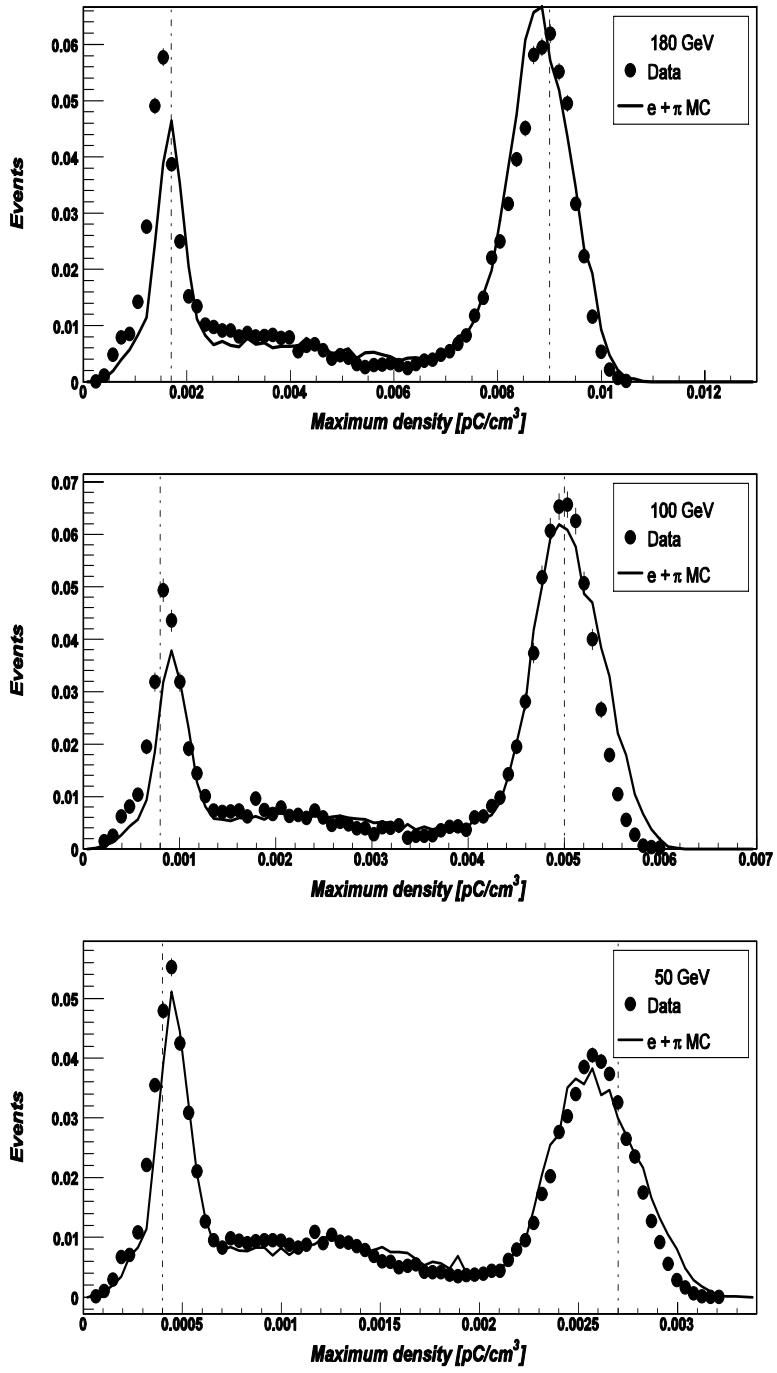

Fig.3 Normalized distribution of maximum energy density for 180 (a), 100 (b) and 50 (c) GeV runs.

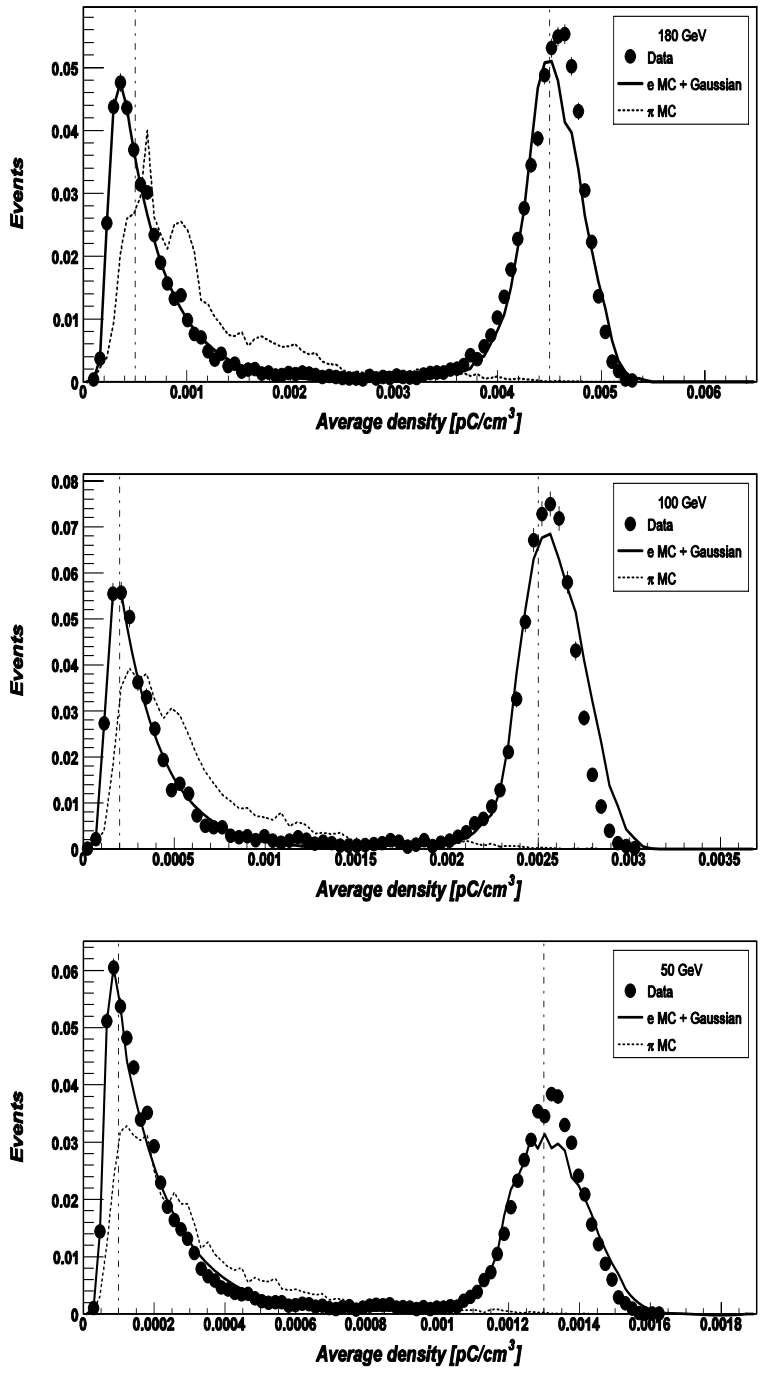

Fig.4 Normalized distribution of average energy density for 180 (a), 100 (b) and 50 (c) GeV runs.

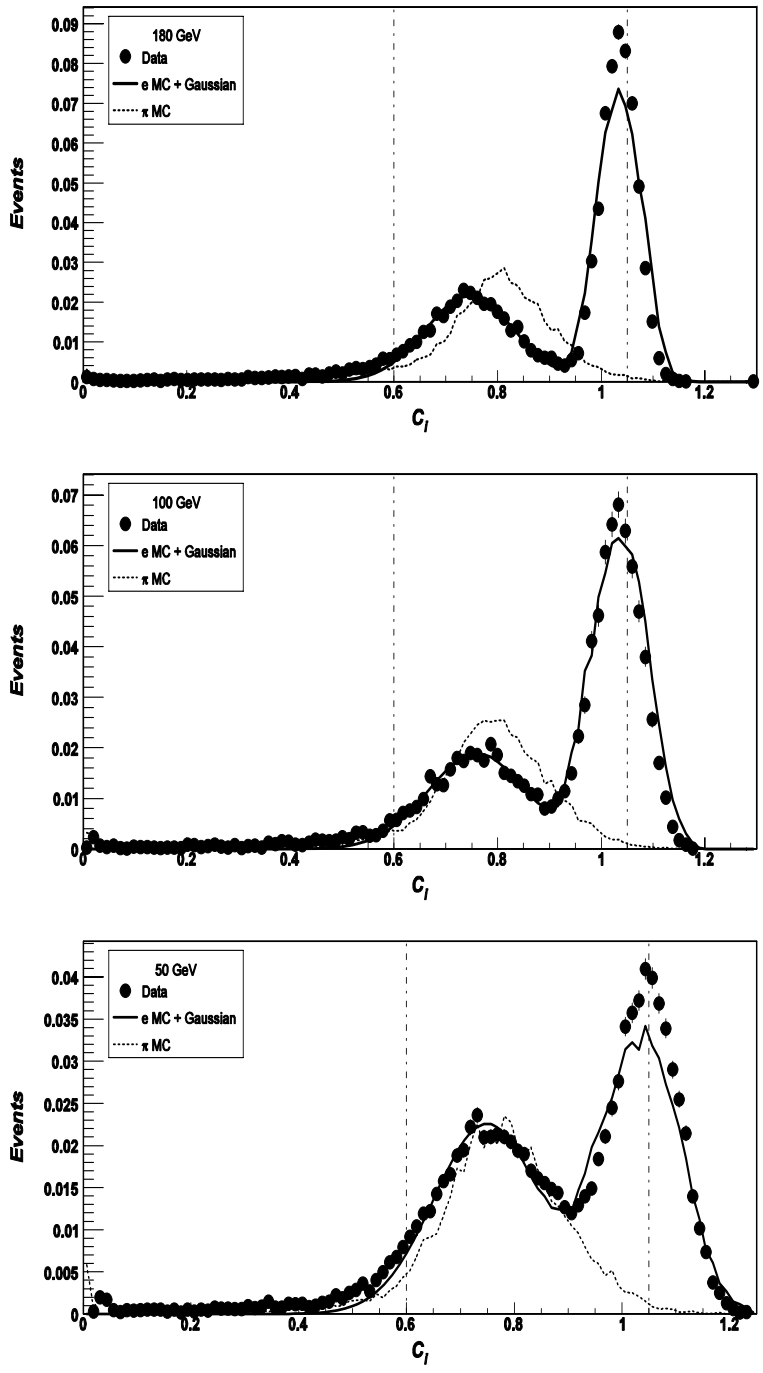

Fig. 5 Normalized distribution of C_i for 180 (a), 100 (b) and 50 (c) GeV runs.

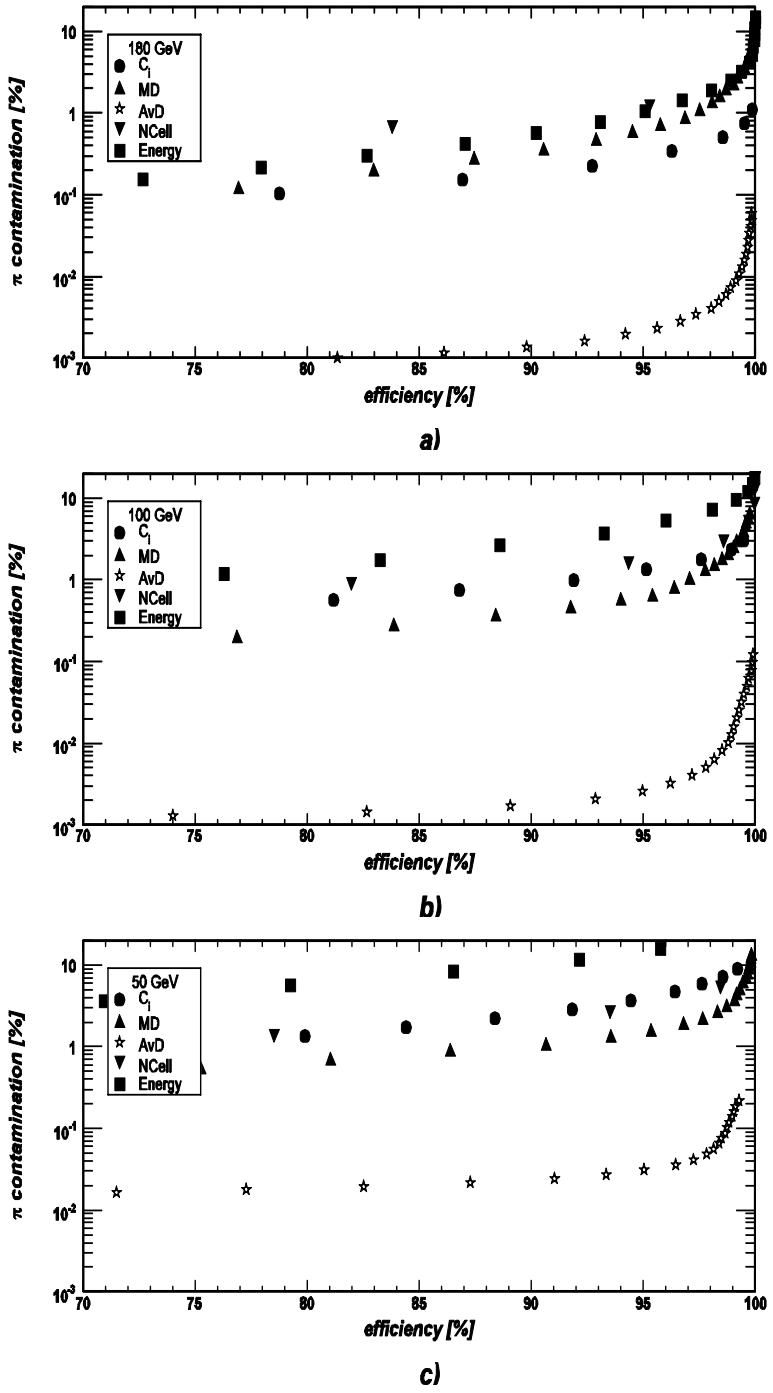

Fig. 6 Electron separation efficiency vs. contamination of pions for 180 (a), 100 (b) and 50 (c) GeV runs.

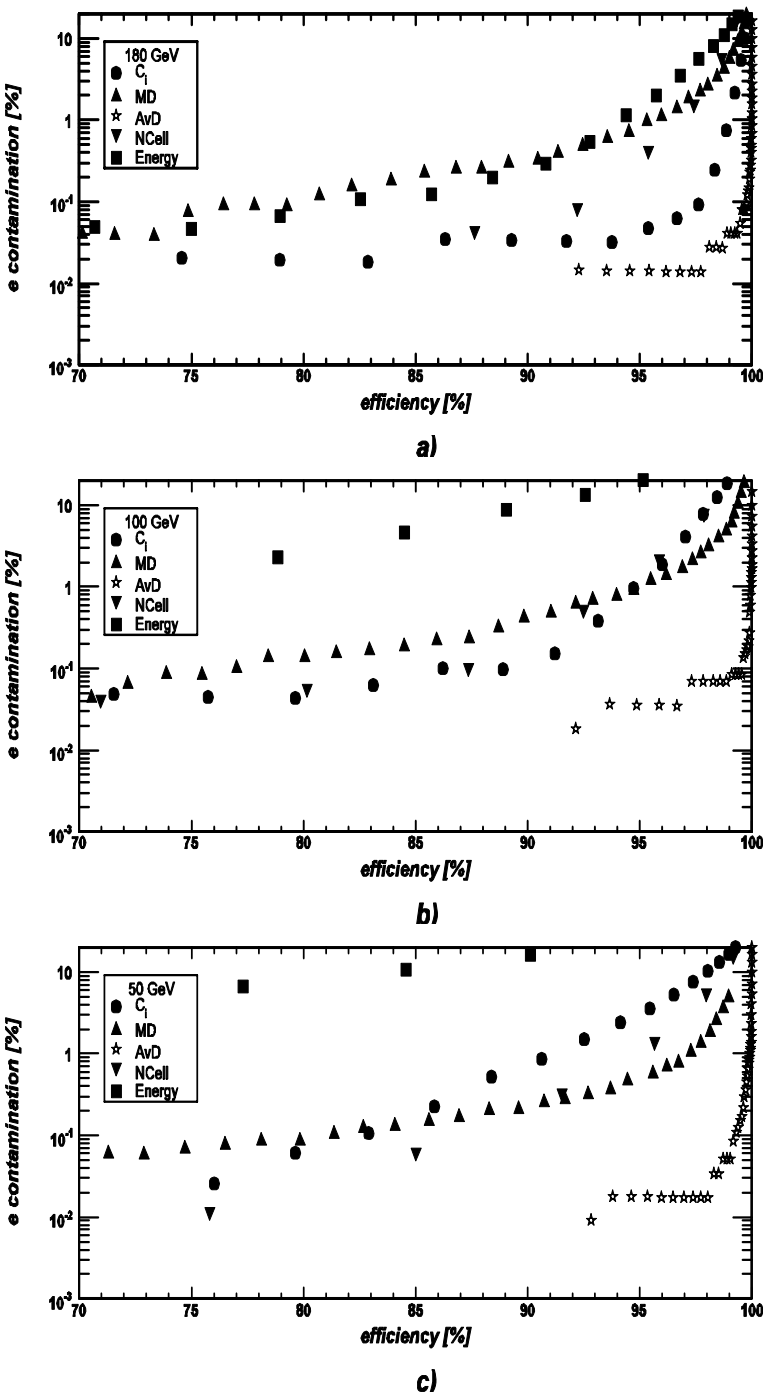

Fig.7 Pion separation efficiency vs. contamination of electrons for 180 (a), 100 (b) and 50 (c) GeV runs.

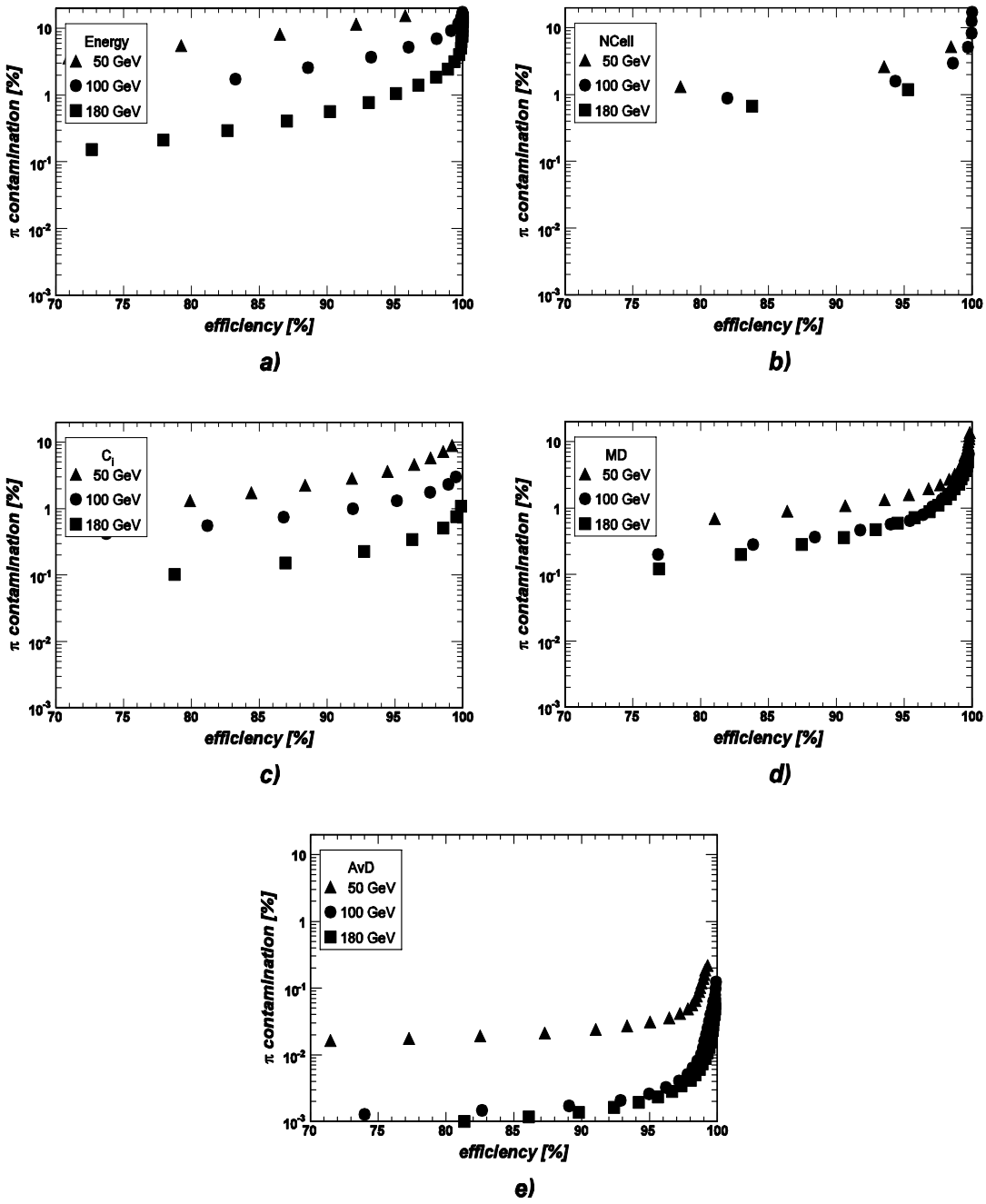

Fig.8 Electron separation efficiency vs. contamination of pions for different energies by the following observables:
a) energy, b) number of cells, c) C_i,
d) maximum energy density, e) average energy density

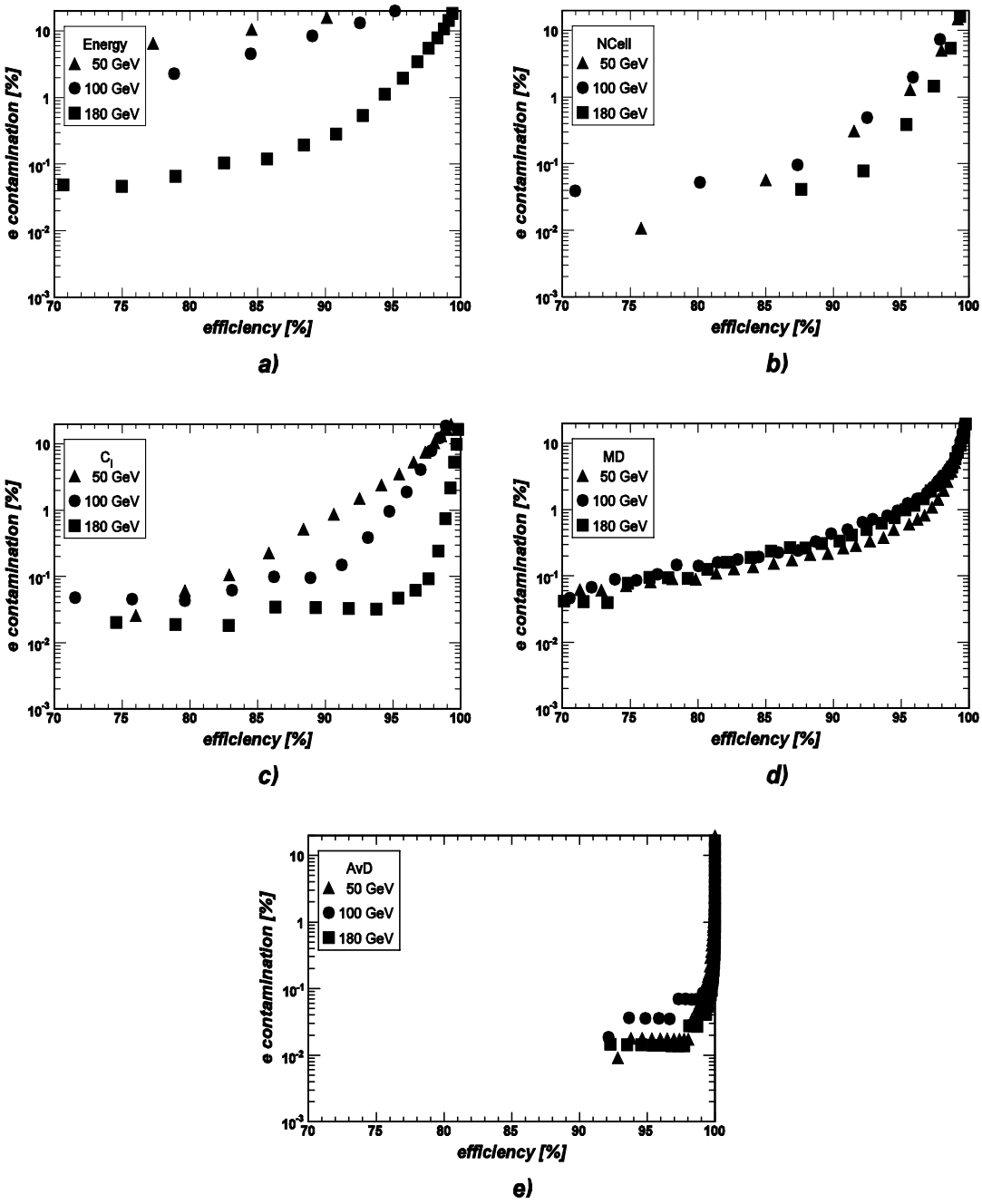

Fig. 9 Pion separation efficiency vs. contamination of electrons for different energies by the following observables:
a) energy, b) number of cells, c) C_i,
d) maximum energy density, e) average energy density